MPPT Technique
For Partially Shade Photovoltaic Module
A Graph Laplacian Approach

Thesis submitted in partial fulfillment of the requirements for the degree of

Master of Technology

in

Electrical Engineering

(Specialization: Control & Automation)

by

Amit Kumar Pandey

Department of Electrical Engineering
National Institute of Technology Rourkela
Rourkela, Odisha, 769008, India

May 2015

MPPT Technique
For Partially Shade Photovoltaic Module
A Graph Laplacian Approach

Dissertation submitted in

in May 2015

to the department of

Electrical Engineering

of

National Institute of Technology Rourkela

in partial fulfillment of the requirements for the degree of

Master of Technology

by

Amit Kumar Pandey

(Roll 213EE3310)

under the supervision of

Prof. Somnath Maity

Department of Electrical Engineering
National Institute of Technology Rourkela
Rourkela, Odisha, 769008, India

Department of Electrical Engineering
National Institute of Technology Rourkela
Rourkela-769008, Odisha, India.

Certificate

This is to certify that the work in the thesis entitled ***MPPT Technique for partially shade Photovoltaic module:A Graph Laplacian Approach)*** by ***Amit Kumar Pandey*** is a record of an original research work carried out by him under my supervision and guidance in partial fulfillment of the requirements for the award of the degree of Master of Technology with the specialization of **Control** & **Automation** in the department of **Electrical Engineering**, National Institute of Technology Rourkela. Neither this thesis nor any part of it has been submitted for any degree or academic award elsewhere.

Place: NIT Rourkela
Date: May 2015

Prof. Somnath Maity
Professor, EE Department
NIT Rourkela, Odisha

Acknowledgment

First and Foremost, I would like to express my sincere gratitude towards my supervisior Prof. Somnath maity for his advice during my project work. He has constantly encouraged me to remain focused on achieving my goal. His observations and comments helped me to establish the overall direction of the research and to move forward with investigation in depth. He has helped me greatly and been a source of knowledge.

I extend my thanks to our HOD, Prof. A.K Panda and to all the professors of the department for their support and encouragement.

I am really thankful to my batchmates especially Pramisha, Ankit, Anupam, and Rahul who helped me during my course work and also in writing the thesis . Also I would like to thanks Mahendra sir for his personal and moral support. My sincere thanks to everyone who has provided me with kind words, a welcome ear, new ideas, useful criticism, or their invaluable time, I am truly indebted.

I must acknowledge the academic resources that I have got from NIT Rourkela. I would like to thank administrative and technical staff members of the Department who have been kind enough to advise and help in their respective roles.

Last, but not the least, I would like to acknowledge the love, support and motivation I recieved from my parents and therefore I dedicate this thesis to my family.

Amit Kumar Pandey
213EE3310

Abstract

One of the topology that comes under distributed control architecture in photovoltaic application is differential power processing. This topology is basically a minimal power processing technique as the differential convertors used here provide mismatch current to the series connected PV module string. Series connected PV module suffers from mismatch problem due to different level of insolation, shading, or manufacturing variation of different sub-module as the current in series connection is same thus the efficiency of the PV system is compromised even when a single sub-module is damaged or solar irradiation is not uniform. This distributed architecture uses bidirectional buck-boost convertor to enable the power flow from one module to another in either direction depending on the opening and closing of Mosfet switch which drive the convertor in buck or boost mode. The control algorithm used to achieve true MPPT is an iterative process which uses local voltage measured and neighbor to neighbor communication to update the algorithm and thus efficient tracking. This architecture overcomes the problem of the conventional power electronics solution for series connected PV module with mismatch, where there is a compromise between system efficiency and total power production. Since the differential convertor deals only with the mismatched power which is just a small fraction of total power and all convertors having same efficiency the overall efficiency can be improved significantly. If there is no mismatch between the modules then ideally no power loss will occur in DPP convertor and the efficiency of system is limited by central invertor. This algorithm uses graph Laplacian approach where Laplacian matrix is used to obtain information from neighboring PV module. This approach reduces the number of iterations at each step thus improving the tracking speed with no added hardware making it more suitable for long series string PV module. Algorithm along with simulation and its properties are presented in this paper.

Contents

List of Figures

List of Abbreviations

AM	:	Air mass
BDC	:	Bi-directional Buck Boost Converter
CSP	:	Concentrated Sun Power
D	:	duty cycle
DC	:	Direct Current
DPP	:	Differential Power Processing
IGBT	:	Insulated Gate Bipolar Transistor
MOSFET	:	Metal Oxide Semiconductor Field Effect Transistor
MPP	:	Maximum Power Point
MPPT	:	Maximum Power Point Tracking
PV	:	Photo voltaic
P&O	:	Perturb and Observe
RECC	:	Returned Energy Current Converter
SOC	:	State of Charge
UPS	:	Uninterrupted Power Supply

Chapter 1

Introduction

Chapter 1

Introduction

1.1 Background

Renewable energy is obtained from natural process and it involves sunlight, wind/tides, geothermal etc which are replenished naturally. Renewable energy has been in use before the development in coal as wind energy was used for sailing the ship, biomass was used for fire. Although the utilization of solar energy for producing voltage goes back to 1839 by Edmund Becquerel it was not until early 1950s when technology for producing highly pure crystalline silicon was developed that the era for PV cells heralded. Solar energy can be used in different forms with the emerging technological innovations like solar photo−voltaic, concentrated sun power, solar heating. There are two methods for obtaining electricity from sunlight, photo−voltaic is a direct method and is highly researched upon method. The other method is an indirect one and is called concentrated solar power (CSP). In this method large area of sunlight is focused using lenses, mirror and trackers on small area thus the concentrated sunlight is used to produce heat energy which is further used to obtained electricity through thermoelectric process. The regions which have high solar insolation are suited for these CSP plant. The worldwide capacity of installed CSP is around 3.4GW [1] with Spain and United States leading in this technology. In photo−voltaic when the junction of a p-n junction diode is illuminated, the number of electron hole pair increases and thus the current is increased as these carrier sweep across the junction. The electron crossing the junction from p to n will flow out through n terminal toward p terminal

when an external circuit is connected, and thus the device behaves as voltage cell. Thus light energy is directly converted into electricity by using photo−voltaic cell. Advancement in transistor technology resulting from huge amount of research and development expended in it has enormously impacted the PV industry as both are made of same material sharing the same physical phenomena. Recent years has seen the growth of PV industry by 60

1.2 Literature Review

A number of architecture has been presented which implement the technique of differential power processing. Some of the topology using minimal power processing are given below: Shuffling converter also called differential power processing Returned energy current converter (RECC) with feedback control Feed forward current control The above circuit topology merits and high level analysis has been given in [3]. Earlier approach which employ a generation control circuit [4] requires a complex gate driving circuit. In this the MPPT slows down as number of PV modules increases as the switch current and voltage rating increases also the circuit complexity increases as the communication between each DPP converter and central converter require extra wires. This will make the implementation more difficult and impair the effort to miniaturization of the system. Also the reliability is limited for this system as a malfunctioning in central unit of communication can render the system useless. But the advantage of generation control circuit is that there is no need of local current measurement thus preventing extra cost and also loss due to current sensing. Other method which is being used recently in photo−voltaic is voltage equalization [5,6] operation. In this method the primary concern of the converter is to maintain the voltages of all the module at same. This method will achieve near MPPT as it will be only effective when the variation in V-I characteristics is small i.e the shading or irradiance variation in very low and the maximum power point voltage sensitivity is less compared to current. DC optimizer [7–9] along with Micro-inverters [10,12] comes under full power processing architecture. In this type of architecture the distributed converters which

are used to implement the algorithm are connected in series to PV string. In DC optimizer the whole power is processed twice, once in DC/DC converter stage and again at central inverter stage. This will result in significant loss in the system as the efficiency is limited by converter and inverter efficiency both. In case of Micro-inverter the PV sub-module is directly connected to the inverter but this architecture has cost disadvantage over central inverter or string level inverter, also the efficiency of the system is compromised as high voltage inverters are more efficient but here inverters are connected to individual sub-module. The topology proposed in is transformer coupled using voltage equalization method as discussed above. To obtain voltage equalization the distributed converters are operated in open loop which will eliminate the need for communication thus simplifying the architecture. But the problem with this is that it requires PV modules with negligible power variation which is not possible generally. Costly binning process [13] is performed during manufacturing where the modules with specific maximum percentage tolerances are grouped together to as to minimize the output power variation, even then also in real time scenario during field operation the voltage of PV module can drift apart due to thermal gradient. One recent approach [14] implementing the distributed algorithm where communication is reduced but instead current is measured for each sub-module causing additional power loss apart from synchronization between converters. From above literature we see that for DPP converters, to obtain the information of neighboring module require communication or local current sensing. The current sensing technique is avoided for the sake of system efficiency and cost. Communication is used between adjacent modules to obtain their voltage, but this should be limited to overcome the central approach.

1.3 Motivation

In photo-voltaics the basic building block is a solar cell which will produce very meager amount of power output. To increase the power output for any practical application group of cells connected together in series parallel arrangement to form

array. Ideally all the PV sub-modules should produce same power output so that overall output is maximized, but it is not so due to various factors influencing external and internal to PV module themselves. In series connected PV module the string current should be same, but due to varying amount of irradiation on different PV module each module has different current and voltage causing a mismatch problem. Thus all the modules cannot produce maximum power simultaneously even if there is no shading because of other factors like manufacturing variability, ageing etc. The power output of PV system is thus seriously hampered by above mismatch problem and this motivates to study distributed sub-module level MPPT.

1.4 Contribution of the Thesis

The objective of this work is to study a distributed algorithm that works on sub-module level and gives true MPPT. Algorithm works on differential power processing [27] architecture which work on providing the series PV string with the mismatch current. The above architecture helps in reducing the size of overall PV system and cost and also improves the power conversion efficiency. Here we want to study a system where low voltage converter is employed and is using minimum communication and no current sensing. In this work PV model has been simulated and also bidirectional buck-boost used as Differential power processing (DPP) converter are designed and simulated in open loop. Some of the salient points of this thesis are:

1. Study of photo-voltaic module and simulation in Mat lab simulink.
2. Study of minimal power processing structure and full power processing architecture.
3. study of the Differential power processing algorithm characteristics .
4. Study of Bi-directional buck boost converter and steady state analysis.

1.5 Organization of the Thesis

The thesis work has been organized as follows:

- **Chapter 2:**This chapter provides the overview of solar photo-voltaics and effects of shading on power output of PV system.
- **Chapter 3:** provides an overview of the various Differential power point architecture and specifically DPP architecture is studied
- **Chapter 4:** in this chapter, Bi-directional buck boost converter is studied and steady state analysis has been studied.
- **Chapter 5:** presents the simulation results and the analysis along with future work and conclusion.

Chapter 2

Modeling of Photo Voltaic Module

Chapter 2

Modeling Of Photo Voltaic Module

2.1 Introduction

The growth of solar cell industry in recent times have been attributed to increasing global warming and uncertainty in climatic conditions due to excessive use of convention fuel and its exploitation. To overcome this problem research have been undertaken at huge pace to move from conventional fuel to renewable energy resources to tap into this inexhaustible source. Thus photo voltaic comes into picture, transforming sunlight into electricity. The benefits that can be achieved from photo voltaic can be given as

- This system contains no moving part so no fear of wear and tear thus preventing maintenance cost.
- Is renewable so no fuel required.
- Is made from Silicon one of the most abundant element on earth.
- Once carefully manufactured and installed requires little maintenance.
- Supports wide range of applications from remote residential use to large scale centralized energy farms.

Apart from these benefits, there are also some con also like it is not reliable due to its dependence on insolation and temperature which are variable. Even

though sunlight is abundant but it is in very dilute form due to scattering and absorption and reflection back in space.Sun releases huge amount of energy beyond usage reach of human need. Per second power output that is produced is 3.86 1020 MW. The amount of sunlight that is available at earth surface is related to quantity of air mass (AM) through which light passes. Atmosphere works as a good filter absorbing large quantity of suns radiation almost 50%. Sun radiation is scattered by small gaseous molecules which are very much smaller than the wavelength of radiation, this type of scattering is known as Rayleigh scattering. Of all the radiation coming into the atmosphere after this Rayleigh scattering process approximately half of it reflects back into space and remaining is diffused to earth. The dust particles which are larger than the wavelength of radiation also scatter the radiation this is known as Mie scattering and it depends on location and dust particles in the atmosphere. The solar spectrum with different molecules absorbing different wavelength is shown in Figure 2.1 [**?**]. All the above factors described

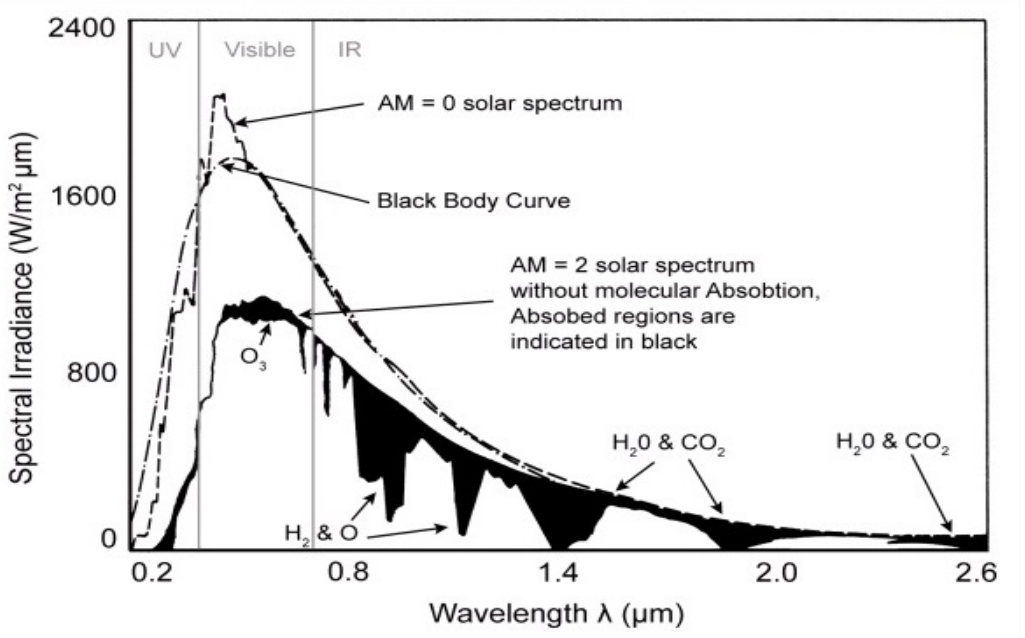

Figure 2.1: The extraterrestrial solar spectrum ($AM0$), ideal black body curve and solar spectrum at the earths surface ($AM2$)

above influence the power output of PV cell. Though the Sun is constant source of irradiation but at earth surface the distribution of irradiation is not uniform thus a good PV system should be modeled taking into consideration these effect.

The present theoretical understanding of photo voltaic has been laid by Quantum mechanics in 1920s and 1930 and major breakthrough was the development of Czochralski method to obtain highly pure Silicon crystal. In 1958 small solar cell array was used in U.S Vangaurd space satellite to power the radio which worked so well that the development of solar cell technology has been part of Space program ever since. The extensive research and development in transistor industry has revolutionized the PV cell technology as both are made of same material and their working depends on same physical phenomena.

2.2 PV cell modeling

The photo voltaic effect can be described as, when solar radiation is incident on PV cells then photons with energy high enough to strike out the electron from valance bond of semiconductor material thus producing electron hole pair which will enable flow of electricity in external circuit and is proportional to light falling on the PV cell. The building block of photo voltaic system is a solar cell which is made of p-n junction photo diode. A group of cells when combined forms a panel or module and when the group of modules are connected in series/parallel arrangement they form an array. When considering small load like light bulb or DC motor the load can be directly connected to photo voltaic (PV) array. Converters are used in other applications where current and voltage from PV has to be regulated to obtain maximum power yield, and to track maximum power point (MPP). From the equivalent circuit we see that when we short circuit the cell, the current will flow through the external circuit, and when the cell is open circuited the diode connected in parallel to PV module will shunt the circuit internally. Hence when we consider open circuit characteristic of the cell, it is set by the diode characteristic. It determines the V-I characteristics of PV cell. Following factor should be considered when we want to obtain the characteristics accurately.

- The reverse saturation current of the diode I0 is temperature dependent.

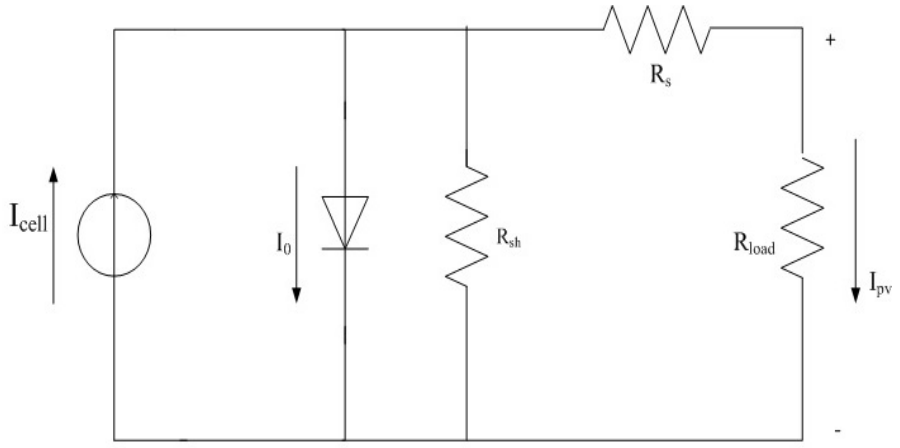

Figure 2.2: Equivalent model of PV cell

- Photo current obtained through the PV array is also temperature dependent.
- Series resistance R_S.
- Parallel resistance R_{sh} connected in parallel to the diode.
- Diode ideality factor η.

The mathematical model of the PV cell is given in equation (2.1)-(2.4), [15]-[17]. Module photo current I_{cell} is given by,

$$I_{cell} = [I_{sc} + K_I(T_{op} - 298)] \times \frac{\lambda}{1000} \tag{2.1}$$

Module reverse saturation current,

$$I_{rev\_sat} = \frac{I_{sc}}{[exp(\frac{qV_{oc}}{N_s K A T_{op}}) - 1]} \tag{2.2}$$

Module saturation current I_0 dependence on temperature is given by,

$$I_0 = I_{rev\_sat} \times [\frac{T_{op}}{T_{ref}}]^3 exp[\frac{q \times E_{g0}}{B \times K}\{\frac{1}{T_{ref}} - \frac{1}{T_{op}}\}] \tag{2.3}$$

The current output of the PV module is given by,

$$I_{PV} = N_p \times I_{cell} - N_p \times I_0[exp\{\frac{q \times (V_{PV} + I_{PV} \times R_s)}{N_s A K T_{op}}\}] \tag{2.4}$$

Following data has been considered as reference to simulate the PV model in Mat lab Simulink. These specifications [26] are given for the standard test

condition for temperature of 250C and irradiance of $1000w/m^2$.

Table 2.1: Electrical characteristics of SOLKAR $36W$ PV Module

Power rating of the module	37.08 W
Maximum power Voltage	16.56 V
Maximum power Current	2.25 A
I_{sc}, Short circuit current	2.55 A
V_{oc}, open circuit Voltage	21.24 V
No of cells in series, N_s	36
No of cells in parallel, N_p,	1
n, Diode ideality factor	1.6

One of the problem that drastically limit the power output is shading of PV module. The shading of a particular PV cell will reduce the current output of that cell and the entire string current will be limited by lowest module current thus when group of cells are connected in series to increase the voltage and hence power then the shaded cell will limit the overall power of PV system. One other problem associated with shading is Hot-spot formation. When overall module current increases than the short-circuit current of shaded cell or group of cell in the same module then the shaded module becomes reversed biased which leads to power dissipation and local overheating. To overcome the effect of partial shading bypass diodes are standard addition to photo voltaic module. These diode function is to provide current path in the circuit when the cell becomes faulty and open circuit, this will enable the module to provide output power even in the case of partial shading but at reduced voltage. To mitigate the effect of partial shading there can be four solutions:

- Modified MPPT techniques

- Interconnection of PV module in different array configuration.
- Different converter topology
- Different PV architecture

2.3 Maximum Power Point Tracking (MPPT)

MPPT is done to obtain maximum power output from the PV module at a given irradiation and temperature condition. In applications where load needs more power than produced by the PV module then power converters can be used to increase the output as required. There are many approach to get the maximum output using MPPT and the choice of MPPT depends on various factors which include Implementation complexity, cost, response time, and ability to detect local and global MPP etc. in case of uniform insolation there is only a single MPP and conventional techniques like perturb and observe *P&O* [18]-[19], hill climbing[20], Incremental conductance [21],[22].

When some cells or sub-module comes under partial shading then these conventional techniques to maximize power are not very effective due to multiple peaks created in the P-V characteristics. These peaks formed because of bypass diode used to prevent hot spot and these local maxima are mistaken for global maxima by these technique. Effective MPPT technique must be used to obtain global peak power and utilize the modules to best of their efficiency. Here in this topic *P&O* algorithm is used to maximize the current and voltage individually in separate loop and with the help of this information DPP converter are used to run the main algorithm which will seek true MPPT.

2.3.1 Perturb and observe technique *P&O*

P&O technique and hill climbing method has gathered much focus among all the conventional MPPT techniques. Fundamentally both method are same but are approached from different way. The operating voltage is perturbed in case of *P&O* method and in case of hill climbing technique duty ratio perturbation is

done which in turn will change the PV array current and thus array voltage. From the PV curve it can be seen that when the voltage is below VMPP and is increased (decreased) then the power also increases (decreases) and in case the operating voltage is to the right of VMPP then increasing the voltage decreases the power and vice-versa. So according to this *P&O* technique if power is increasing then the perturbation direction should be same as before but if the power decrease, direction of perturbation should be reversed. This process should be repeated till maximum power is obtained. There is one drawback of this algorithm is that there is oscillation around the maximum power point and it depends on the step size of the perturbation. If the step size is reduced oscillation can be reduced, but the MPPT will slow down. Summary of MPPT technique using *P&O* is given below in Table 2.

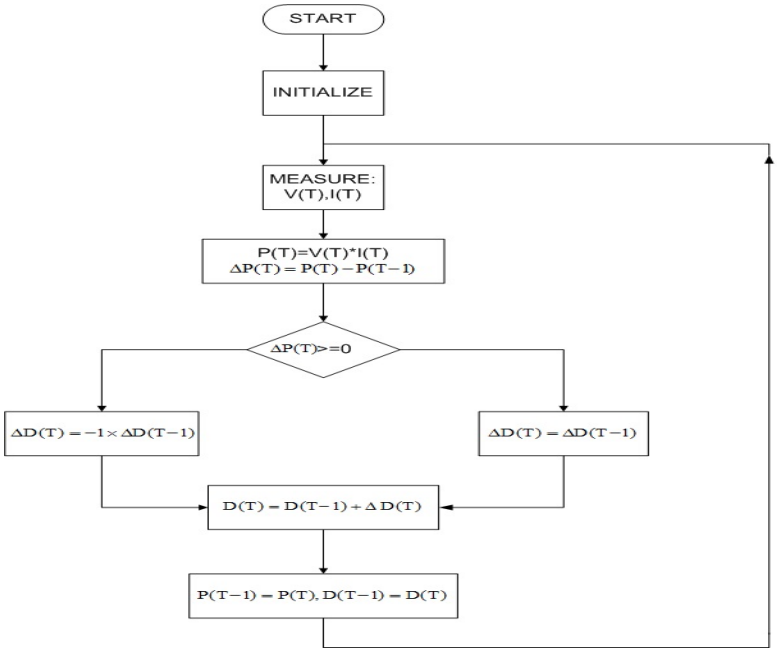

Figure 2.3: Flow chart for *P&O* algorithm

The flow chart for *P&O* algorithm is given in Fig 5 [**?**]. One another disadvantage of this algorithm is that in case sudden variation in atmospheric condition this method fails to recognize the true maximum power point. If the atmospheric condition vary between one sampling interval the P-V curve changes, the operating point will change between that and algorithm will not recognize true MPP.

Chapter 3

Differential Power Processing

Chapter 3

Differential Power Processing

3.1 Introduction

Generating the power that can be used in any application or standalone PV system high voltage is needed so connection of PV cells are done in series this will increase the overall voltage across the module and to increase the current these modules are connected in parallel. This type of connection is often prone to mismatch due to variation of irradiation temperature aging etc which will cause the current of affected module to differ from other resulting into mismatching. Due to power loss it is not possible to determine the operating point at which the system operates at maximum power point. To rectify this problem different kinds of architecture are used which perform module level MPPT. These are also referred to as distributed MPPT architecture. Distributed architecture can be categorized into two types

- Full power processing architecture
- Minimal power processing architecture

Dc optimizer and micro-inverters are two types of full power processing architecture as these process the full power obtained from their PV module regardless of the irradiation.The block diagram of both these architecture is shown in Figure 3.2(a) and 3.2(b) [10] In case of minimal power processing architecture [22] very small amount of power is processed. Bulk power is directly fed to central inverter and the dc/dc converter only process on the difference of power between adjacent

modules. Advantages of minimal power processing are

- Reduced converter rating
- Low losses
- Converter operating under lower stress.

Disadvantage of minimal power processing are

- Complex MPPT algorithm
- Complex wiring connections

In case of DC optimizer high efficiency converters which are able to sustain themselves should be designed. The advantage with these converter is that they can independently track the maximum power and control them locally. This is done by connecting converter to each panel which results in PV panels that are independent of system complexity and its geometry. This system is intelligent, low cost and is reliable. These converter are able to switch its operation between three modes that are buck mode, boost mode and pass-through mode. Output of converter is directly connected to input in case of pass-through mode and there are minimum losses at nominal condition. Using MIC the string voltage is regulated to fixed value and this will enable low cost and optimized design and size of converter adding reliability to system. The advantage of this configuration is that PV panels are decoupled from each other and the string thus they can operate at their individual maximum power point and unaffected from variation in string current

In minimum power processing architecture and full power processing architecture the location of MPPT unit might be confusing as one cannot easily determine if closed loop regulator is to be used or an MPPT should be applied. The basic difference between these two methods is that in case of MPPT it is an iterative process of obtaining the maximum power point using the algorithm while in case of closed loop regulator negative feedback is used to fix the current or voltage

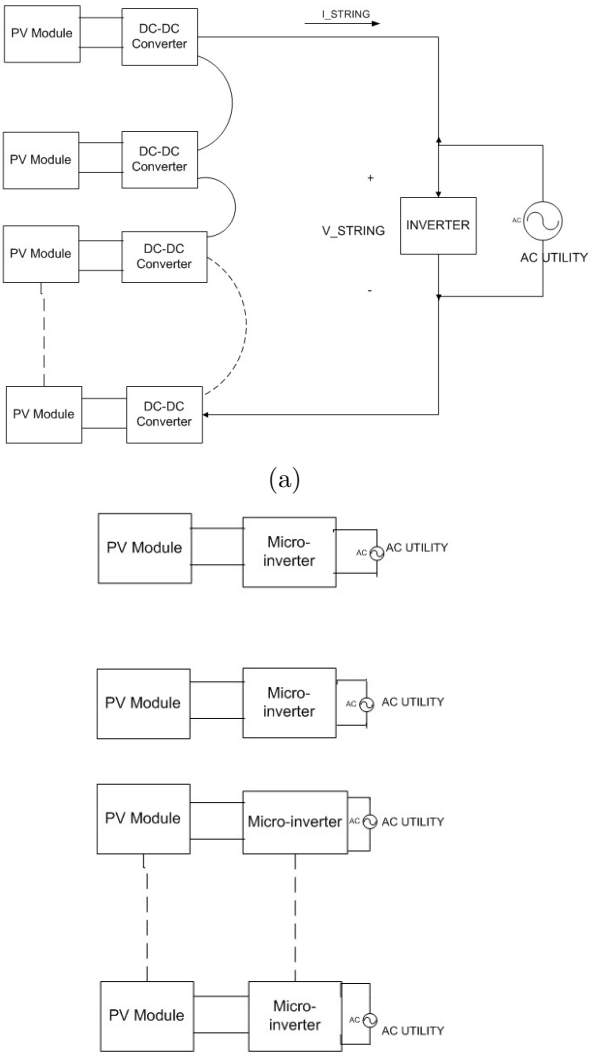

Figure 3.1: (a)DC optimizer Architecture and (b)Micro-Inverter Architecture

at a reference value. The number of Power processors that are used to regulate the operating point and degree of freedom was identified for power system was presented by theorem in [23]. In the theorem it was concluded that the system operating point should be equal to number of converters used to control it. If the above conclusion is applied for distributed architecture then following Lemma 1 was given in [**?**] Lemma 1: A system with N photo voltaic module must contain exactly N maximum power point tracking unit (MPPT). In case of minimal power processing this guideline is not intuitive. In this architecture the inverter should

have MPPT unit for itself. The closed loop regulator will not be able to obtain the exact maximum power. The string power including the converter is maximized by PV module maximum power point and the string voltage is sum of all the module voltages. Thus the power and voltage both are maximized at string output by MPP of PV module. This will lead to determination of string current as both power and voltage is known.

The number of MPPT unit for string should be equal to (N-1) for N number of PV module as one MPPT unit will be dedicated to inverter. Increasing or decreasing the number of MPPT unit will either result in instability and deadlock or reduced power harvested.

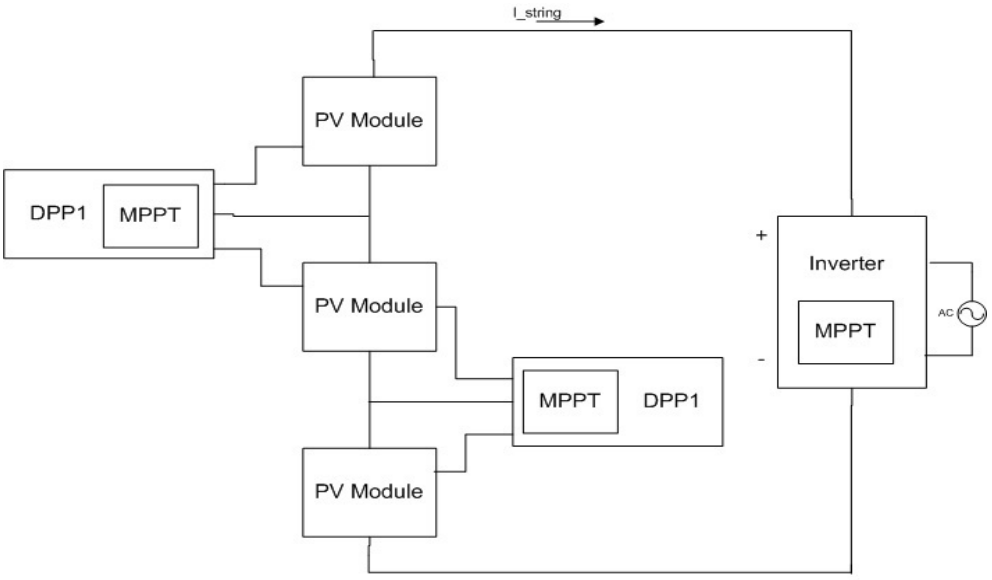

Figure 3.2: Adequate DPP Architecture with MPPT location

3.2 DPP Architecture for 3 sub-module 2 DPP system

In this architecture 3 sub-modules are connected in series and DPP converters are connected between pair of sub-modules. The architecture [27] is shown in Figure 3.3(a) . This architecture can be scalable to large number of PV modules and DPP converters. The necessity of the system is to improve the efficiency and

one important factor is to operate the converter only when it is necessary and with as minimal possible power that is required. It enables the series connected PV module to work at MPP by providing the difference of current between the two adjacent PV modules as shown in Figure 3.3(b) [**?**] conceptually. In case of no mismatch the converter will provide no current to series PV circuit and there will be no power exchange. The bulk power is directly sent to central inverter without processing it through DPP converters which will reduce the converter rating as it will only have to pass required differential power and hence there will be low losses and improved efficiency of the overall system. The size of the converter will also be reduced as it will be working at very high frequency and the inductor size will be small. As shown in Figure 3.3(b) the string current of 2A has to be maintained so that there is no mismatch. As the modules are connected in series they have their own VMPP and IMPP so they needed to be matched to common string current which is done by DPP converters.

The system consist of DPP converters which are basically bi-directional converter connected in parallel to the string of series PV module which are then connected to central converter as shown in Figure 3.3(a). The objective here is to maximize the power obtained from the series connected module. To achieve this objective of MPPT two control loops are considered for current and voltage. In current loop the central inverter is configured as controllable current sink which will be used to maximize current using perturb and observe algorithm. In other loop the overall voltage of the sub module is maximized by adjusting the duty ratio of Differential converters again using perturb and observe algorithm. It is worth noting that the time constant of DPP converter is much smaller than that of perturbation time for current loop. Considering any current I, it can be seen that irrespective of irradiation condition the voltage can be maximized which is equivalent to power maximizing.

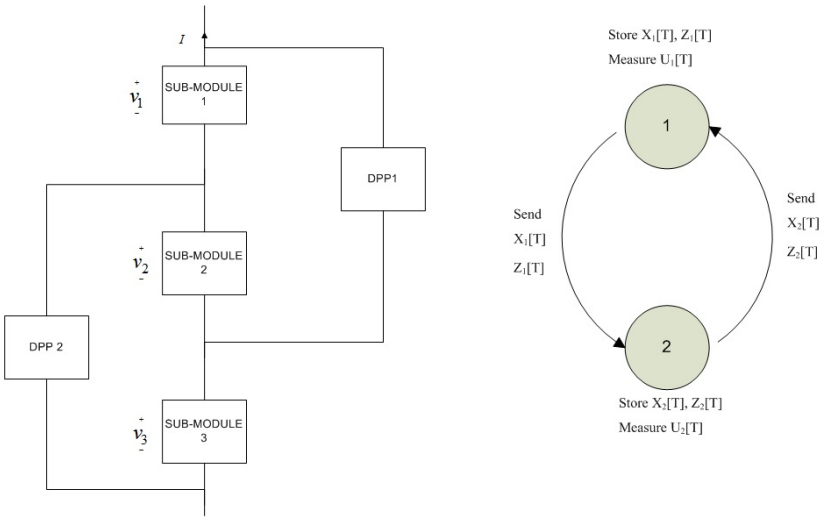

(a)

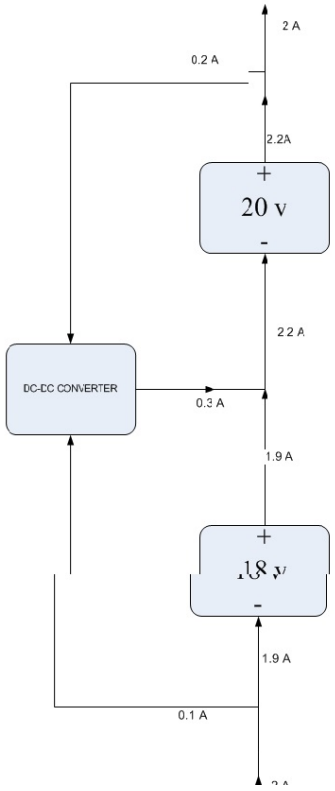

(b)

Figure 3.3: (a)DPP Architecture with information exchange between neighbors and (b)DPP example showing current matching

The control algorithm along with equations(3.1) − (3.7) [27] is given as ,

$$maxV(D_1, D_2) = v_1(D_1, D_2) + v_2(D_1, D_2) + v_3(D_1, D_2) \tag{3.1}$$

D_1 and D_2 are duty ratio of DPP_1 and DPP_2. The maximum of function can be obtained by setting its gradient to zero

$$\nabla V(D_1^*, D_2^*) = \begin{bmatrix} \frac{\delta v_1}{\delta D_1} + \frac{\delta v_2}{\delta D_1} + \frac{\delta v_3}{\delta D_1} \\ \frac{\delta v_1}{\delta D_2} + \frac{\delta v_2}{\delta D_2} + \frac{\delta v_3}{\delta D_2} \end{bmatrix} = \begin{bmatrix} 0 \\ 0 \end{bmatrix}$$

D_1^* D_2^* are respective duty ratio corresponding to maximum power. The optimal value of duty ratio is obtained by local controllers which will adjust the value of D iteratively based on:

- Measured local voltage
- State variables maintained by local controller
- Variables which are estimated by neighboring DPP

The differential converters will maintain a state variable which will be determined locally.

$$x[T] = [D_1[T], \hat{D_{1,2}}[T], \hat{D_{2,1}}[T], D_2[T]]^T \tag{3.2}$$

$$z[T] = [z_{1,1}[T], z_{1,2}[T], z_{2,1}[T], z_{2,2}[T]]^T \tag{3.3}$$

The variables are updated after each iteration as:

$$x[T+1] = (I_4 - \delta\tilde{L})x[T] - \delta\tilde{L}z[T] + \delta\gamma u[T] \tag{3.4}$$

$$z[T+1] = z[T] + \delta\tilde{L}x[T] \tag{3.5}$$

Where $D_1[T]$ is actual duty ratio of DPP1,$D_2[T]$ is actual duty ratio of DPP2,$\hat{D_{1,2}}[T]$ is DPP1s estimate of duty ratio of DPP2.$\hat{D_{2,1}}[T]$ is DPP2s estimate of duty ratio of DPP1, and $Z_1[T]$ and $Z_2[T]$ are ancillary state vector maintained by local controller. I_4 is 4×4 identity matrix and $\tilde{L} \bigotimes I_2$, where I_2 is 2×2 identity matrix. $\bigotimes$ denotes Kronecker product of L and I_2.

$$L = \begin{bmatrix} 1 & -1 \\ -1 & 0 \end{bmatrix}$$

L is Laplacian matrix of graph representing exchange of information between local controllers shown in Fig 3.3 (a). δ and γ are tuning parameters used for tuning the algorithm. $u[k]$ is defined as:

$$u[T] = \begin{bmatrix} [\frac{\delta\psi_1}{\delta D_1}]|_{D_1[T],D_2[T]} & [\frac{\delta\psi_1}{\delta D_2}]|_{D_1[T],D_2[T]} & [\frac{\delta\psi_2}{\delta D_1}]|_{D_1[T],D_2[T]} & [\frac{\delta\psi_2}{\delta D_2}]|_{D_1[T],D_2[T]} \end{bmatrix}^T$$

ψ_1 and ψ_2 are defined as:

$$\psi_1(D_1, D_2) = v_1(D_1' D_2) + \frac{1}{2} \times v_2(D_1, D_2) \tag{3.6}$$

$$\psi_2(D_1, D_2) = v_3(D_1' D_2) + \frac{1}{2} \times v_2(D_1, D_2) \tag{3.7}$$

From above equations it can be observed that the update of DPP1 states is function of its own state, state of neighbor and partial derivative of input function $u[T]$. The information that will be used to update the algorithm will be obtained with the help of N2N communications. To perform this estimation at every iteration DPP perturb its duty ratio by fixed small amount while both local controller observes the sub-module voltage and after receiving the required information they update their respective states. After sufficiently large no. of iterations string voltage is maximized. The timeline for the control algorithm is shown in Figure 3.4 [27].

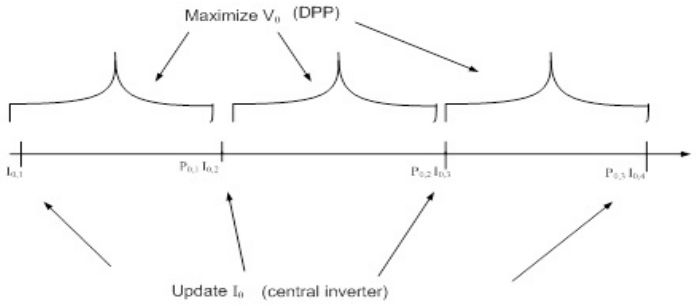

Figure 3.4: Timeline for slow and fast control loop

From the time line we can see that first the slow control loop is initiated as

the central inverter will update a certain string current and then in second control loop the DPP will run the control algorithm to maximize the voltage output of series string which will be sum of all the voltages of module and thus the overall maximum power can be extracted for that particular current which will be used in *P&O* algorithm in next iteration. The value of current is then perturbed to next value and DPP converter again maximize the voltage and we get a power for this value. The difference between this power obtained and power for the previous value of current drives the direction of next current perturbation. From the architecture it is observed that each DPP module is connected to a pair of PV module thus it has information of module which are adjacent to it through local controllers of DPP. Neighbor to neighbor (N2N) communication is used by the controllers to obtain the duty ratio which maximizes overall voltage of the module. The flow chart [27] for algorithm is given in the Figure 3.5.

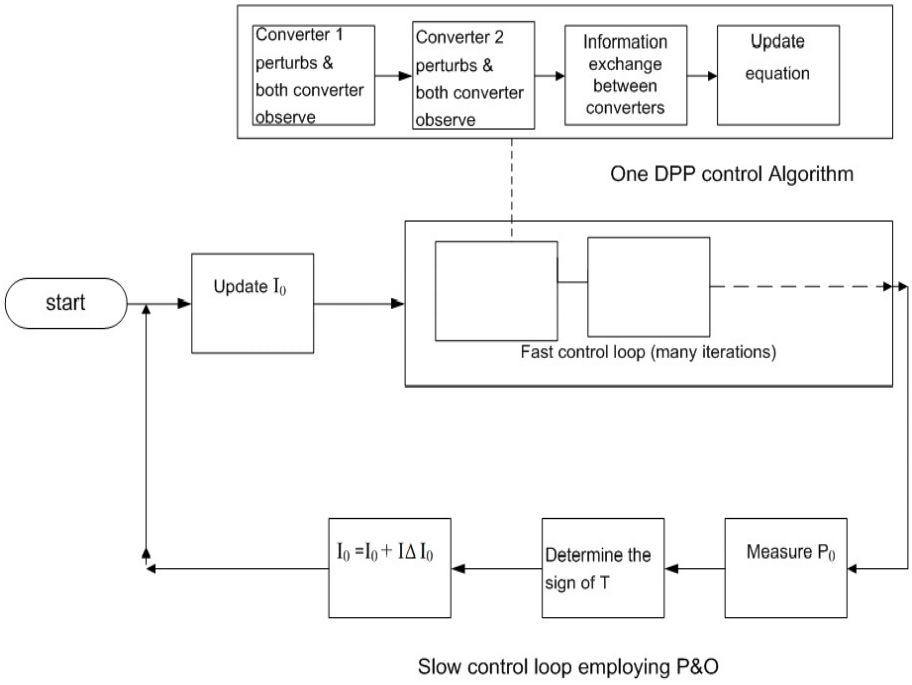

Figure 3.5: Simplified flowchart describing the working of algorithm

3.2.1 Algorithm extension for N sub-module (N-1) DPP system:

The studied algorithm is scalable to large number of PV modules and the state vectors along with ancillary vectors are given in equation (3.8) – (3.13) [27],

$$x[T] = [x_1[T]\ x_2[T]\ ...\ x_i[T]\ ...\ x_{n-1}[T]]^T \tag{3.8}$$

$$z[T] = [z_1[T]\ z_2[T]\ ...\ z_i[T]\ ...\ z_{n-1}[T]]^T \tag{3.9}$$

The local controller of differential converter maintain these state vectors. These controllers have role of maintaining the duty ratio estimate of its own state and the estimate of duty ratio of neighbors.

$$x_i[T] = [\hat{D_{i,1}}[T]\ ...\ \hat{D_{i,i-1}}[T], D_i[T], \hat{D_{i,i+1}}[T]\ ...\ \hat{D_{i,n-1}}[T]]^T \tag{3.10}$$

$$z_i[T] = [z_{i,1}[T], z_{i,2}[T],\ ...\ z_{i,n-1}[T]]^T \tag{3.11}$$

Where,

$$u[T] = \left[\frac{\delta\psi_1}{\delta D} \quad [\frac{\delta\psi_2}{\delta D} \quad .... \quad \frac{\delta\psi_{n-1}(D)}{\delta D}\right]^T$$

$$\frac{\delta\psi_i}{\delta D} = \left[\frac{\delta\psi_i}{\delta D_1} \quad [\frac{\delta\psi_i}{\delta D_2} \quad .... \quad \frac{\delta\psi_i(D)}{\delta D_{n-1}}\right]^T$$

$$\psi_i(D) = \begin{cases} v_i(D) + \frac{1}{2}v_{i+1}(D), & i = 1 \\ \frac{1}{2}v_i(D) + \frac{1}{2}v_{i+1}(D), & 1 < i < n-1 \\ \frac{1}{2}v_i(D) + v_{i+1}(D) & i = n-1 \end{cases}$$

$$x[T+1] = (I_{n-1^2} - \delta\tilde{L})x[T] - \delta\tilde{L}z[T] + \delta\gamma u[T] \tag{3.12}$$

$$z[T+1] = z[T] + \delta\tilde{L}x[T] \tag{3.13}$$

I_{n-1^2} is $(n-1)\times(n-1)$ identity matrix. The Laplacian matrix for this configuration

is given as

$$L = \begin{bmatrix} 1 & -1 & 0 & ... & ... & 0 \\ -1 & 2 & -1 & 0 & ... & 0 \\ 0 & -1 & 2 & -1 & ... & ... \\ ... & ... & ... & ... & ... & ... \\ ... & ... & ... & -1 & 2 & -1 \\ 0 & ... & ... & ... & -1 & 1 \end{bmatrix}$$

The same case is arrived as with that for 3 PV module and 2 DPP converter. After sufficient number of iterations the optimum value of duty ratio is observed.Although the Laplacian matrix and the update function are in matrix form, but the computation is distributed. The distributed approach can be explained when considering node 1, DPP updates and store the vectors $x_i[T]$ and $z_i[T]$ which is part of equation (3.8) and (3.9). The information of the neighboring module will be provided by the Laplacian matrix and when considering the i_{th} row of that matrix, it will give DPPis estimate of adjacent module voltages. when only $x_i[T+1]$ is computed by expanding the update function in equation (3.12) and (3.13) we get,

$$x_i[T+1] = \delta x_{i-1}[T]+(1-2\delta)x_i[T]+\delta x_{i+1}[T]+\delta z_{i-1}[T]-2\delta z_i[T]+\delta z_{i+1}[T]+\delta\gamma u_i[T] \tag{3.14}$$

$$z_i[T+1] = z_i[T] + \delta x_{i-1}[T] + 2\delta x_i[T] - \delta x_{i+1}[T] \tag{3.15}$$

From the above equation it is clearly seen that the value of next updated state will depend solely on the information obtained through DPP which will provide the estimate of the closest neighboring through N2N communications.

3.3 Discussion on the characteristics of the studied algorithm:

3.3.1 Choice of tuning parameter γ

The amount of influence that input vector will have on state vector will be determined by this parameter .when the value of γ is large the response will be fast but there will be large overshoot in duty ratio in transient response. When differ-

ent value of γ is used in the update function then the duty ratio the system will evolve with time. When the irradiance changes with time as step function then even with changing values forγ the steady state value to which algorithm converge is same. The overshoot in duty ratio at $t = 0$ is large when compared to other irradiance change at different time. At $t = 0$ the system will get no information from neighboring DPP, thus at cold start the state vectors $x[T]$ can be initialized to 0.5 but $z[T]$ which is taken to support the input vector $u[T]$ will be have to be initialized to 0. For small value of $z[T]$ small γ is preferred as state vector will detect even very small change in input vector and this will suppress the overshoot. This small value will slow down the convergence rate of duty ratio, but it can be considered as tuning of differential processor which will happen just once in a day. After steady state is reached and system converges,γ values should be increased as small value will cause the system to become slow. The increased value of γ will result into effective tracking of irradiance variation. once $z[T]$ reaches steady state large variation in will not cause large overshoot in duty cycle. If the value has to be changed without affecting the duty cycle then some on-line technique have to be used [27]. Once steady state is reached then we have'

$$x[T+1] = x[T] = x^* \tag{3.16}$$

$$z[T+1] = z[T] = z^* \tag{3.17}$$

When the above values are put into update equation then we get,

$$\tilde{L}z^* = \gamma u^* \tag{3.18}$$

$$\tilde{L}x^* = 0 \tag{3.19}$$

From equation (2.24) it is clear that if the value of γ and $z*$ are scaled by same factor then changing the value will not influence the duty cycle as there will be no change in equilibrium point.

Impact of communication topology on convergence speed

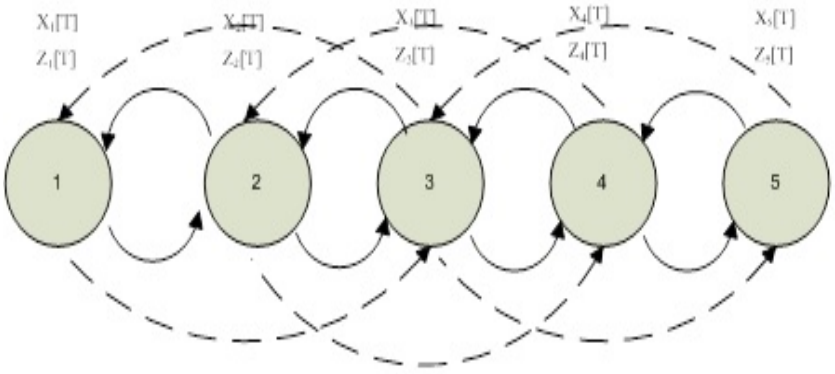

Figure 3.6: Graph of 6 sub-module 5 DPP showing redundant communication

The graph of communication topology is shown in above figure (3.8)/cite27. The solid lines shown represent N2N communication, but this communication will slow down the algorithm for evolving duty cycle. But if the communication will also include immediate neighbor along with one extra neighbor closest to immediate neighbor then there will be redundancy in the system. But this redundancy will increase the convergence speed of the system. This extra connections will be requiring more hardware but there will not be significant impact on control algorithm as there will be only change in the Laplacian matrix which will incorporate this new connections. The Laplacian matrix [27] is given for this communication topology as:

$$L = \begin{bmatrix} 2 & -1 & -1 & 0 & 0 \\ -1 & 3 & -1 & -1 & 0 \\ -1 & -1 & 4 & -1 & -1 \\ 0 & -1 & -1 & 3 & -1 \\ 0 & 0 & -1 & -1 & 2 \end{bmatrix}$$

The advantage of this new connection is that it will greatly improve the convergence speed. When more and more communication links are added then in that case the convergence speed is increased significantly.

3.3.2 Impact of communication topology on reliability:

If the directed graph remains strongly connected then in that case the system will provide optimal solution and converge. When the communication topology of Figure (3.6)/cite27.is considered and connections are made to closest and second closest neighbor then this algorithm can be reconfigured to perform under communication failures. If the failure occur as shown in Figure (3.7). then local controllers will determine the failure and it will reconfigure the Laplacian matrix by changing the corresponding row. The Laplacian matrix [27] can be given as,

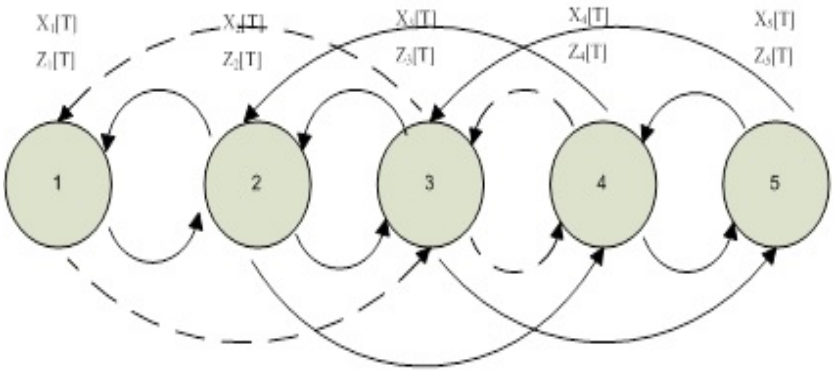

Figure 3.7: Graph for 6 sub-module 5 DPP with Communication failure

$$L = \begin{bmatrix} 1 & -1 & 0 & 0 & 0 \\ -1 & 3 & -1 & -1 & 0 \\ 0 & -1 & 3 & -1 & -1 \\ 0 & -1 & -1 & 3 & -1 \\ 0 & 0 & -1 & -1 & 2 \end{bmatrix}$$

From the Laplacian matrix it can be seen that there is variation in first row and third row rest of the matrix remains unaffected. This change in matrix implies that there is communication failure in DPPs which are on either end of link and is completely local to them only, rest of the system will perform MPPT as usual.

Chapter 4

Bi-directional Buck Boost Converter

Chapter 4

Bi-directional Buck Boost Converter

4.1 Introduction

Earlier when the power flow was required in both directions i.e from source to load and load to source two unidirectional converters were used with each converter processing in one direction. Bi-directional converters were used to overcome the problem of size as these are compact, smaller and have good efficiency and are mainly used in space and telecommunications industry. Traditionally the bi-directional dc-dc converters were used in DC motor drives, but the ability to reverse the direction of current flow and the flow of power has made bi-directional converters an important component in power system like renewable energy, fuel cell and hybrid vehicle also. Multiple input bi-directional converter plays a crucial role when there are many different sources, interconnecting them and managing proper power flow. In renewable energy source like solar and wind, the output power is varying due to fluctuations in atmospheric conditions, but the load should be operated at constant supply so there is need of these converters as they allow auxiliary storage unit to store energy and provide energy to load when DC bus voltage is low. The power flow in both directions is realized by using MOSFET OR IGBT in parallel with a diode as switch with current flow in both direction is not available.

4.2 Bi-directional converters

Bi-directional converters can be categorized into two types:

- Non-isolated Bi-directional converters.
- Isolated bi-directional dc-dc converters.

4.2.1 Non-isolated bi-directional dc-dc converter

The criterion for selecting a non-isolated bi-directional dc-dc converter are size, cost and higher efficiency. For the above said reasons bi-directional converters (BDC) are fancied in spacecraft system and high power system. The basic diagram of bi-directional buck-boost converter is given in Fig 4.1.

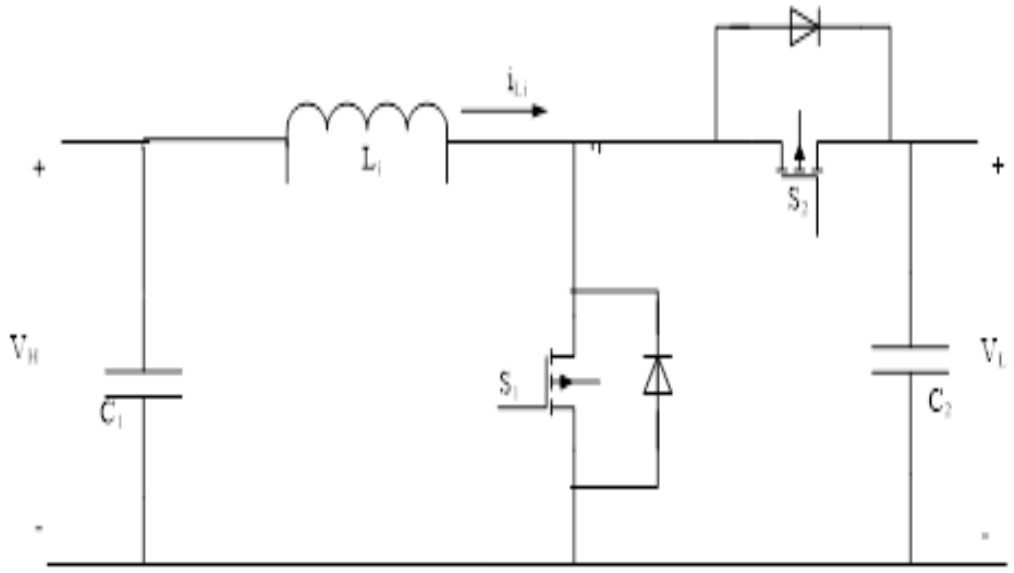

Figure 4.1: Bi-directional buck-boost converter

From the above Fig 4.1, we can see the anti parallel combination of step up and step down stage. The step up operation can be used in motor drive application to increase the battery voltage and controlling of the inverter input. Step down mode is used for regenerative braking allowing braking current to pass and storing of vehicle energy in battery. Increase in power density can be obtained through

current interleaving technology [25]-[26] with minimized inductance.

4.2.2 Isolated bi-directional dc-dc converter

Isolation in BDC is provided by transformer but it incurs additional cost and more losses. Isolation is used in applications which require isolation as well as matched impedance between the isolated circuit. Different topology that comes under this category is a half bridge, full bridge, push pull or their variations. In one of the topology primary side of transformer is half bridge arrangement while secondary side is current fed push pull arrangement [26].This configuration works in two modes, one in which battery is charged using the main bus while battery provides power when dc bus is not available. This type of circuit is used in charging and discharging circuit in UPS. The transformer in isolated converter utilizes leakage inductance as energy storing and transferring element. The full bridge arrangement is considered best among other topology but it complicated having large size and is costly.

4.3 Modeling of Bi-directional Buck-Boost converter

Depending on the power produced by each PV module, this BDC manages the flow of power between two modules by providing small amount of mismatch current thus balancing the current in series circuit. This circuit structure enables the converter to operate in two modes depending on the direction of power flow: buck mode and boost mode.

4.3.1 Boost Mode

The BDC used here is a synchronous circuit i.e complimentary gating signals is used to switch the Mosfet on or off. If switch S1 is ON then S2 will be OFF, both

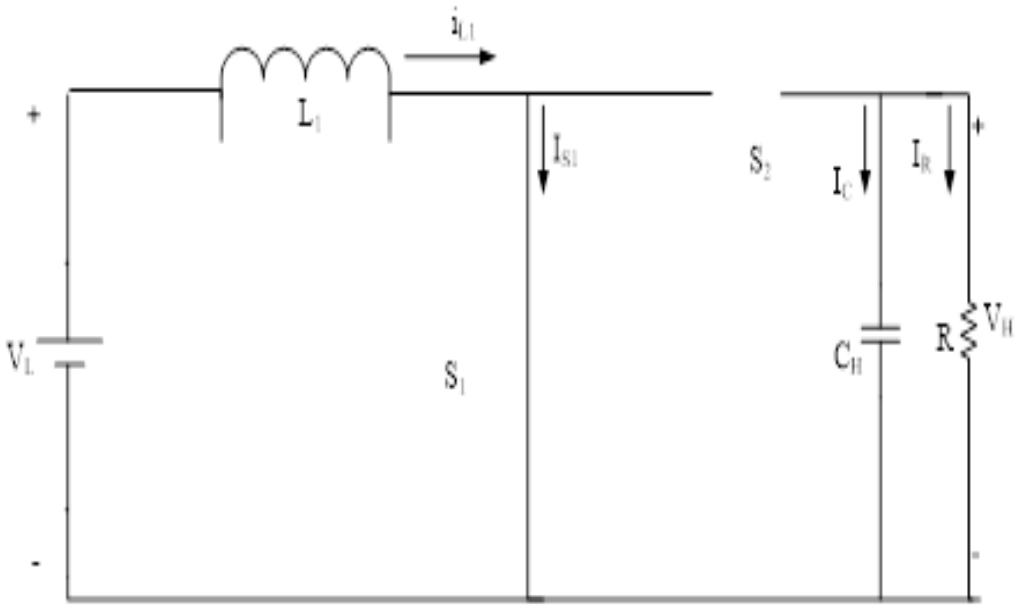

Figure 4.2: BDC in boost mode with switch S1 closed and S2 open

switch cant work in same state simultaneously. Depending on the switch position two operational modes are possible. Duty ratio is defined as ratio of ON time to total time period of the signal.

$$D = \frac{T_{on}}{T} = \frac{T_{on}}{T_{on} + T_{off}}$$

T_{on} is time during which signal is ON or the switch is connected and T_{off} is time when the switch is open. The equations [**?**] given in $(4.1) - (4.39)$ describe the steady state modeleling of the converter.Considering the case of closed switch S1

Closed switch $S1(0 \leq t < DT)$

When the switch S1 is closed then due to complementary operation of switches S2 will be open. The low voltage side supply is connected to inductor L1 and total supply voltage appears across inductor.

$$V_L = L_1 \frac{dI_{L1}}{dt} \tag{4.1}$$

As the voltage across inductor is constant, the inductor current will increase linearly with closed switch S1. The inductor current change is given as

$$\frac{\Delta I_{L1}}{\Delta t} = \frac{\Delta I_{L1}}{DT} = \frac{V_L}{L_1} \tag{4.2}$$

From the above equation (3.2) we see that

$$\Delta I_{L1}(on) = \frac{V_L}{L_1} DT \tag{4.3}$$

Open switch $S1(DT \leq t < T)$

When switch S1 is opened then again due to complimentary action switch S2 is closed. The high side capacitor is connected to load resistor R. the equivalent circuit is shown in Figure.

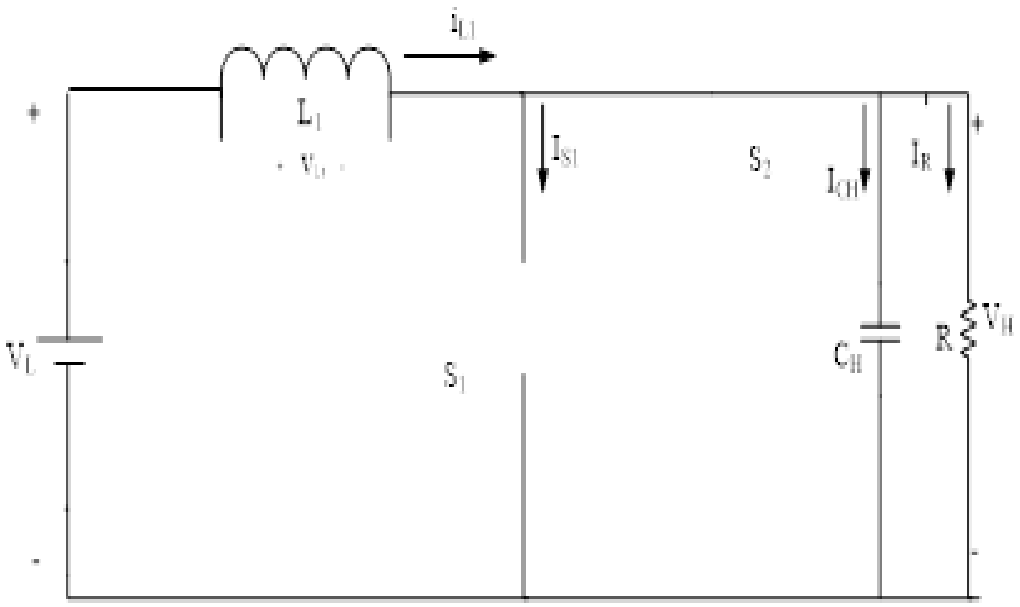

Figure 4.3: Bi-directional converter with switch S1 open and S2 closed

Voltage across inductor is given as

$$v_{L1} = V_L - V_H = L_1 \frac{dI_{L1}}{dt} \tag{4.4}$$

Simplifying the above equation

$$\frac{dI_{L1}}{dt} = \frac{V_L - V_H}{L_1} \tag{4.5}$$

In case of open switch S1 there is linear decrease in change in inductor voltage. It is given as follows

$$\frac{\Delta I_{L1}}{\Delta t} = \frac{\Delta I_{L1}}{(1-D)T} = \frac{V_L - V_H}{L_1} \tag{4.6}$$

Thus from above equation we get

$$\Delta I_{L1}(off) = \frac{V_L - V_H}{L_1}(1-D)T \tag{4.7}$$

At steady state, the sum of inductor current during ON and OFF time should be equal to zero. Thus

$$\Delta I_{L1}(on) + \Delta I_{L1}(off) = 0$$

$$\frac{V_L - V_H}{L_1} + \frac{V_L - V_H}{L_1}(1-D)T = 0 \tag{4.8}$$

The above equation represent inductor volt second balance, and simplifying above equation (3.8) we get,

$$V_H = \frac{V_L}{1-D} \tag{4.9}$$

As the value of D varies between 0 and 1 hence it is clear from equation (3.9) that converter operates in boost mode and voltage VH on high voltage side is greater than that of low voltage side VL

Capacitance design under boost mode

The Boost mode analysis was done based on the assumption that the capacitor on high value side can hold on to any voltage value. But there is variation in voltage at high side due to the effects of limiting capacitance. The variation of charge on capacitors is given as

$$|\Delta Q_H| = \frac{V_H}{R}DT = C_H \Delta V_H \tag{4.10}$$

The ripple voltage is given by

$$\Delta V_H = \frac{V_H}{RC_H} DT = \frac{V_H D}{RC_H f} \tag{4.11}$$

$$C_H = \frac{D}{Rf(\Delta V_H / V_H)} \tag{4.12}$$

Here R is load resistance on high voltage side, f is converter switching frequency, and $(\Delta V_h / V_H)$ is ripple ratio on high voltage side.

Inductance design for boost mode

Input power on both sides of converter should be equivalent if we neglect line losses.

$$V_L I_{L1} = \frac{V_H^2}{R} = \frac{(V_L/(1-D))^2}{R} = \frac{V_L^2}{(1-D)^2 R} \tag{4.13}$$

Thus inductor current is given by

$$I_{L1} = \frac{V_L^2}{(1-D)^2 R} \tag{4.14}$$

The maximum and minimum inductor current is obtained as

$$I_{L1max} = I_{L1} + \frac{\Delta I_{L1}}{2} = \frac{V_L}{(1-D)^2 R} + \frac{V_L}{2I_{L1}} DT \tag{4.15}$$

$$I_{L1min} = I_{L1} - \frac{\Delta I_{L1}}{2} = \frac{V_L}{(1-D)^2 R} - \frac{V_L}{2I_{L1}} DT \tag{4.16}$$

The continuous conduction mode requires that the minimum value of inductor current should be greater than 0. So equation (3.16) must be satisfied

$$\frac{V_L}{(1-D)^2 R} - \frac{V_L}{2I_{L1}} DT \geq 0 \tag{4.17}$$

Simplifying the above equation so that minimum inductor current should be satisfied, the minimum inductance value should be

$$L_{1min} \geq \frac{D(1-D)^2 R}{2f} \tag{4.18}$$

Thus to work in boost mode the bi-directional buck boost converter should

have its inductor current in CCM in any duty cycle

4.3.2 Buck Mode

The converter works under buck mode and is determined by the switch position. Considering the case of closed switch S2 and switch S1 open.

Closed switch $(0 \leq t \leq DT)$

When switch S2 is closed then due to complimentary operation of gating signal switch S1 is open. The equivalent circuit of converter is shown in Figure

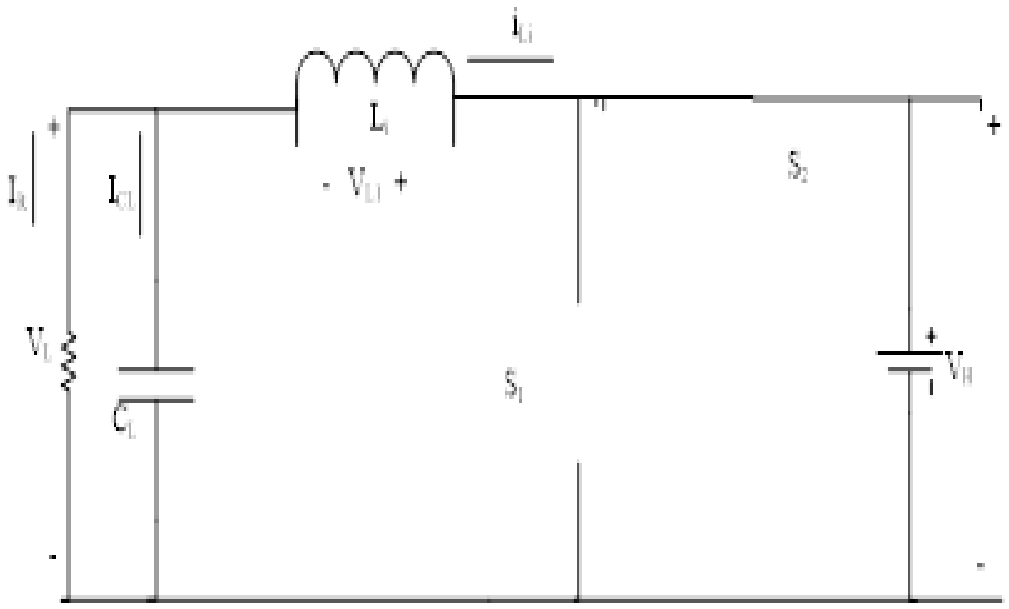

Figure 4.4: converter in buck mode with switch S1 open and S2 closed

The voltage across inductor is given as

$$V_{L1} = V_H - V_L = L_1 \frac{dI_{L1}}{dt} \tag{4.19}$$

Simplifying we get

$$\frac{dI_{L1}}{dt} = \frac{V_H - V_L}{L_1} \tag{4.20}$$

From above equations, positive value of rate of change of inductor current

implies linear increase. The above equation can be written as

$$\frac{\Delta I_{L1}}{\delta t} = \frac{V_H - V_L}{L_1} \tag{4.21}$$

Change in inductor current during the on time is

$$\Delta I_{L1}(on) = \frac{V_H - V_L}{L_1} DT \tag{4.22}$$

Open Switch S2 ($DT \leq t < T$)

Equivalent circuit in case of open switch S2 and closed switch S1 is given in Figure.

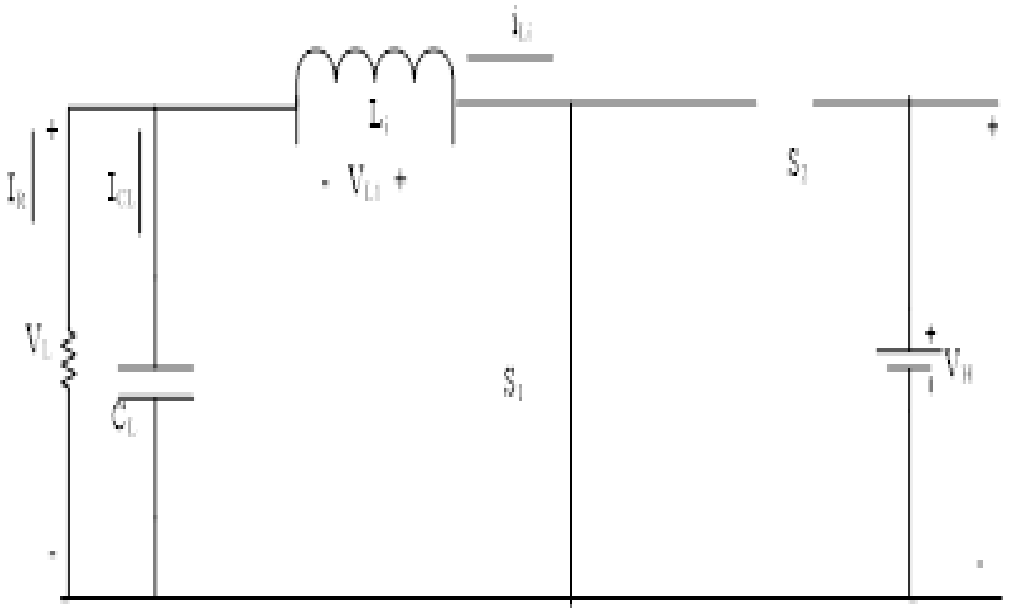

Figure 4.5: Equivalent circuit in case of open switch S2 and closed switch S1 is given in Figure.

Voltage across inductor can be given as

$$V_{L1} = -V_L = L_1 \frac{dI_{L1}}{dt} \tag{4.23}$$

Simplifying the above equation we get

$$\frac{dI_{L1}}{dt} = -\frac{V_{L1}}{L_1} \tag{4.24}$$

The ve sign in above equation signifies that the rate of change of inductor current presents a linear decrease. It can be written as

$$\Delta I_{L1}(off) = -\frac{V_{L1}}{L_1}(1_D)T \tag{4.25}$$

By using inductor volt second balance

$$\Delta I_{L1}(on) + \Delta I_{L1}(off) = 0$$

$$\frac{V_H - V_L}{L_1}DT - \frac{V_L}{L_1}(1_D)T = 0 \tag{4.26}$$

Simplifying above equation, we get

$$(V_H - V_L)DT - V_L(1_D)T = 0 \tag{4.27}$$

Equation (4.27) represents inductor volt-sec balance principle and from above equation only we get

$$V_L = V_H D \tag{4.28}$$

From equation (4.28) it is clear that voltage on low voltage side is lower than voltage high voltage side.

Capacitance design for Buck Mode

The capacitor current is given by as

$$I_{CL} = I_{L1} - I_R$$

We can say from the fig that positive capacitor current implies charging of the capacitor. The change in capacitor charge defines the capacitance and voltage at low voltage side and is given as

$$\Delta Q_L = C_L \Delta V_L \tag{4.29}$$

we can also obtain the solution of above equation, calculating the area under positive capacitor current

$$\Delta Q_L = \frac{T\Delta I_{L1}}{8} \tag{4.30}$$

Comparing equations (4.29) and (4.30) we get

$$\Delta V_L = \frac{T\Delta I_{L1}}{8C_L} \tag{4.31}$$

Incorporating equation (4.25) into (4.31) we get

$$\Delta V_L = \frac{V_L(1_D)}{8C_L L_1 f^2} \tag{4.32}$$

Here f is switching frequency of the converter. The value of capacitance can be formulated as

$$C_L = \frac{(1-D)}{8(\Delta V_L/V_L)L_1 f^2} \tag{4.33}$$

The voltage ripple requirement specified can be used to obtain the capacitance value.

The Inductor design

At steady state the capacitor current is zero, so the mean value of current flowing through capacitor and resistor are same. The mean current is expressed as

$$I_{L1} = I_R = \frac{V_L}{R} \tag{4.34}$$

The minimum value of current through inductor is given as

$$I_{L1max} = I_{L1} + \frac{\Delta I_{L1}}{2}$$

$$I_{L1max} = \frac{V_L}{R} + \frac{1}{2}[\frac{V_L}{L_1}(1-D)T] = V_L[\frac{1}{R_L} + \frac{(1-D)}{2L_1 f}] \tag{4.35}$$

$$I_{L1min} = I_{L1} - \frac{\Delta I_{L1}}{2}$$

$$I_{L1min} = \frac{V_L}{R} - \frac{1}{2}[\frac{V_L}{L_1}(1-D)T] = V_L[\frac{1}{R_L} - \frac{(1-D)}{2L_1 f}] \tag{4.36}$$

The inductor value for CCM is obtained when minimum value of inductor current is equated to zero and minimum inductance is obtained when

$$L_{1min} \geq \frac{(1-D)R}{2f} \tag{4.37}$$

The consistency in bi-directional buck-boost converter for inductor current is

maintained as follows

$$L_{1boost} = \frac{D(1-D)^2 V_H^2}{2P_H f} \tag{4.38}$$

$$L_{1buck} = \frac{(1-D)^2 V_L^2}{2P_L f} \tag{4.39}$$

Here $P_H = \frac{V_H^2}{R}$ and $P_L = \frac{V_L^2}{R}$. The value of D is increased in steps and is substituted in above equation (4.38) and (4.39) to obtain the maximum value solution.

The bi-directional converter has been simulated in MAT-LAB simulink which shows the state of charge of battery, voltage and current at both the terminals of the converter when the duty cycle is changed.

Chapter 5

Simulation and Results

Chapter 5

Simulation and Results

First of all the photo voltaic module is simulated using the specifications given in chapter 2 .The result of simulation run were satisfactory and was as expected.The waveform for V-P,V-I and I-P under different level of irradiation and varying temperature is given as follows:

- current Vs Power characteristics are shown here with varying level of Irradiance.

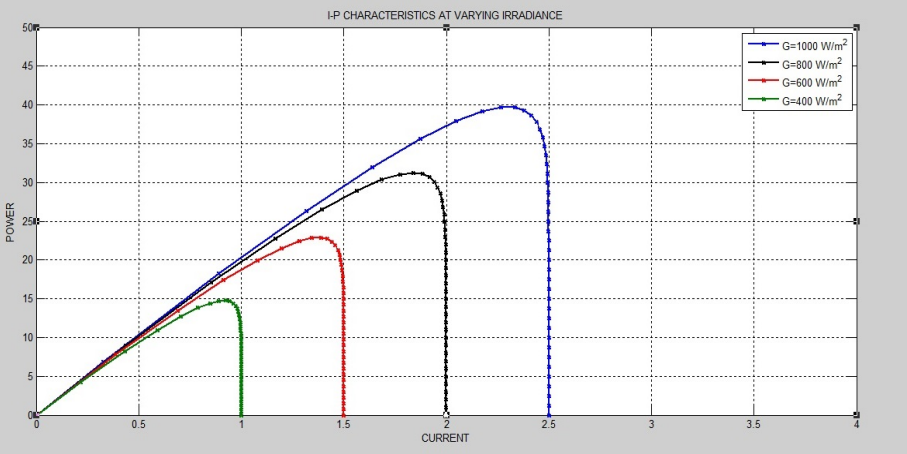

Figure 5.1: I-P characteristics with varying Irradiance

- current Vs Power characteristics are shown here with varying level of temperature.
- voltage Vs power characteristics is shown at varying level of irradiance.
- voltage Vs power characteristics is shown at varying level of temperature.

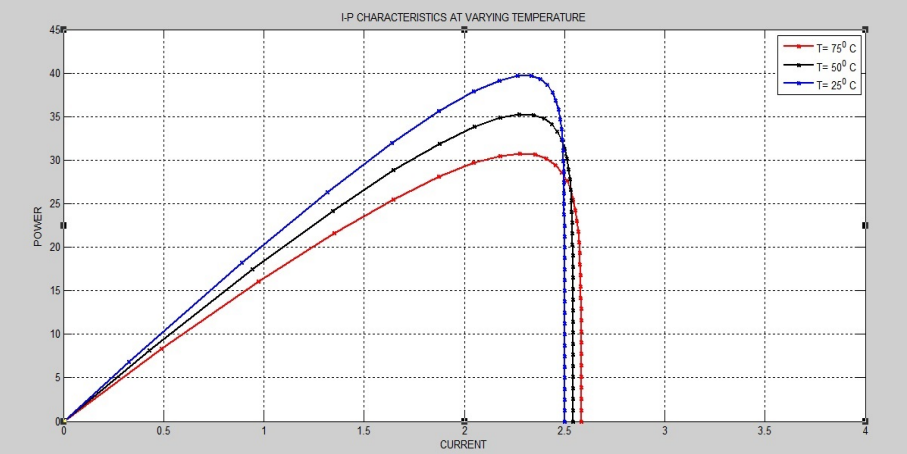

Figure 5.2: I-P characteristics with varying Temperature

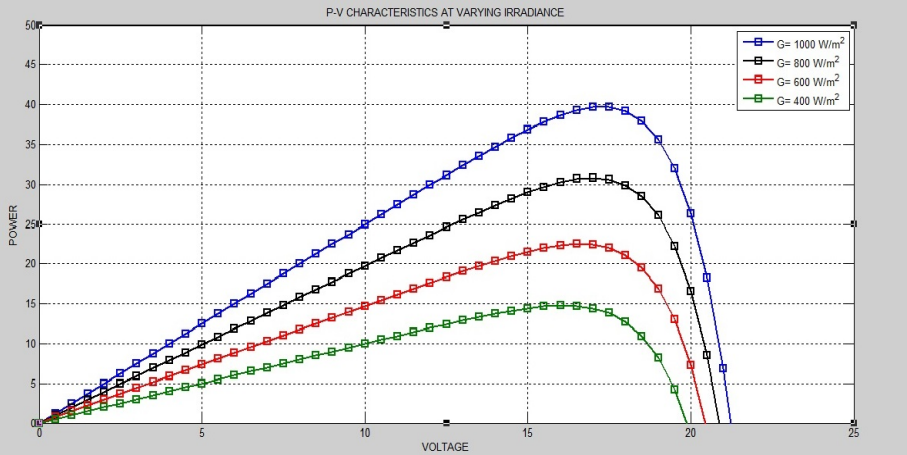

Figure 5.3: V-P characteristics with varying Irradiance

- voltage Vs current characteristics are shown with varying level of solar irradiance.
- voltage Vs current characteristics are shown with varying level of solar temperature.

When the insolation is increased he current output is increased also the voltage obtained is increased. The increased current and voltage results in increased power output

Open loop Bi-directional buck boost converter is modeled in Mat lab Simulink platform. The state of charge (SOC), current and voltage of battery connected at

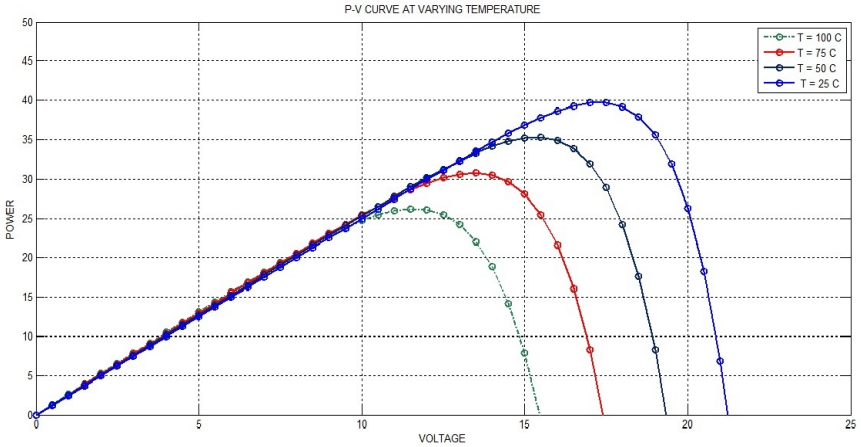

Figure 5.4: V-P characteristics with varying temperature

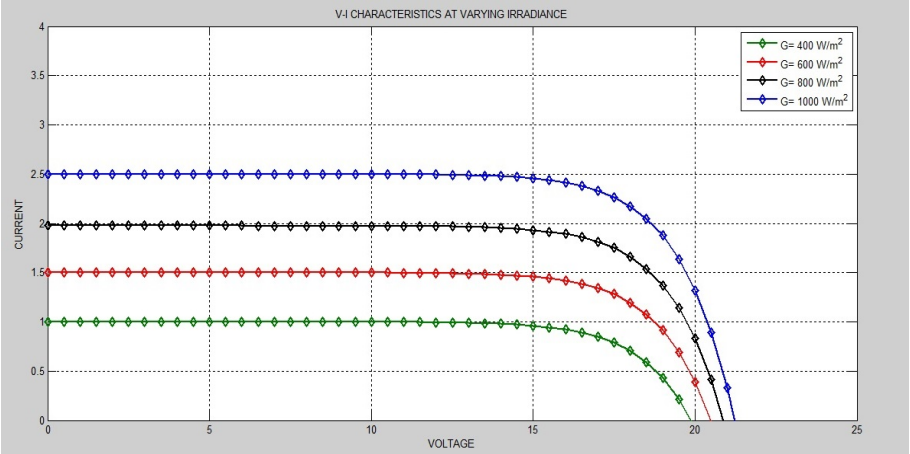

Figure 5.5: V-I characteristics with varying Irradiance

both the terminals are obtained for different duty cycle

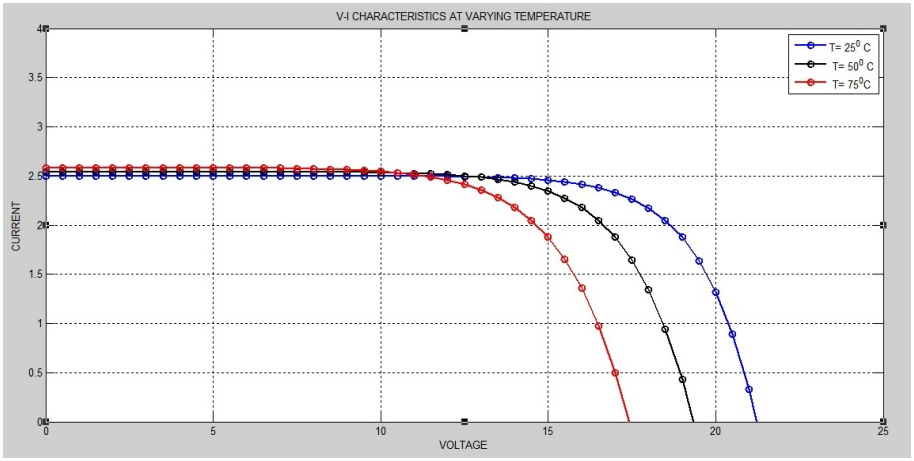

Figure 5.6: V-I characteristics with varying temperature

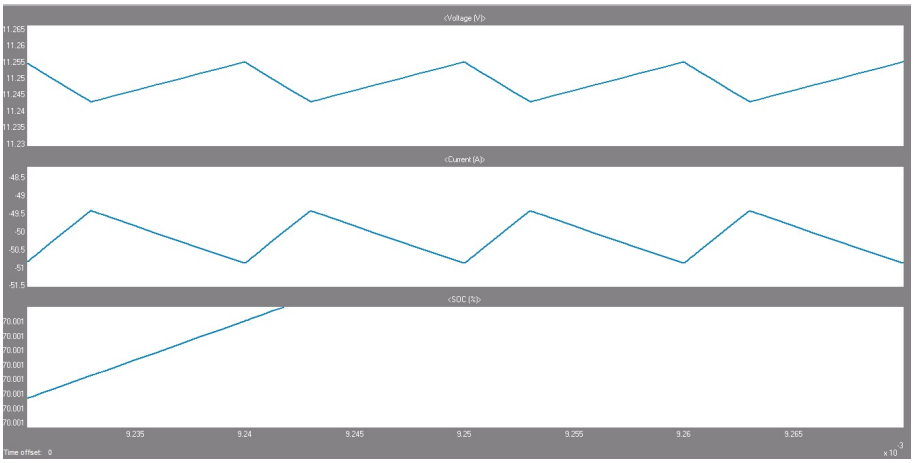

Figure 5.7: Waveform for battery voltage, current and state of charge (SOC) at terminal 1

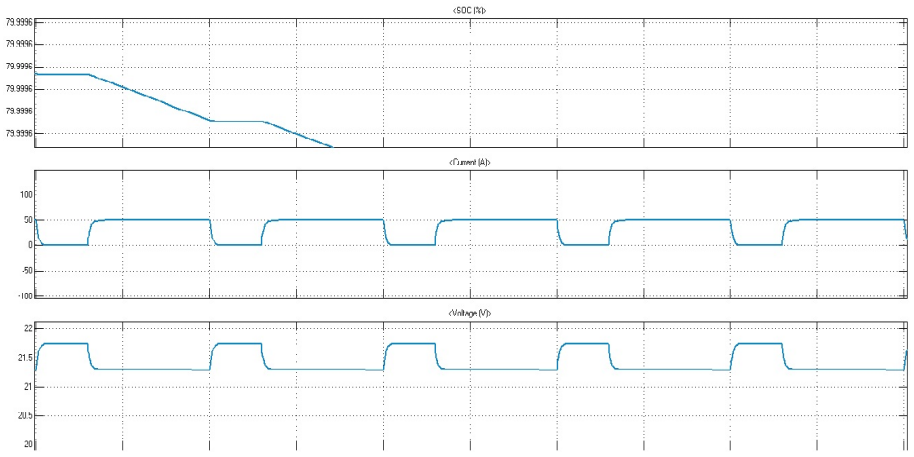

Figure 5.8: Waveform for battery voltage, current and state of charge (SOC) at terminal 2

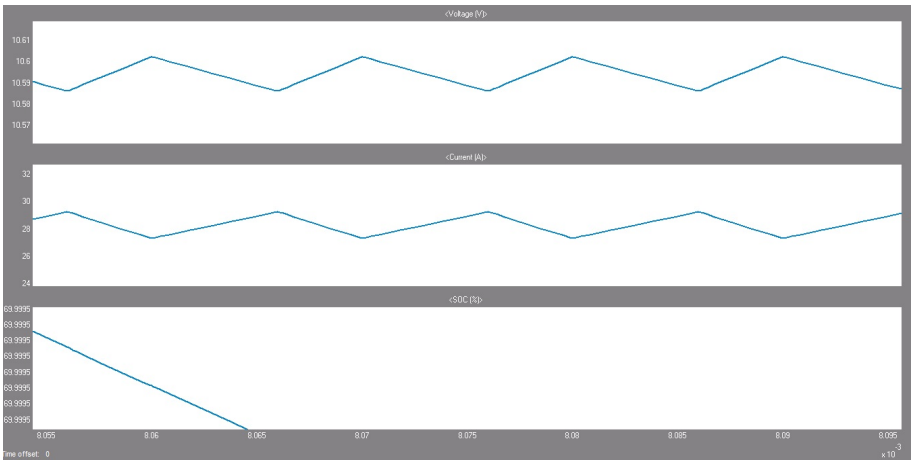

Figure 5.9: Waveform for battery voltage, current and state of charge (SOC) at terminal 1 when duty ratio is changed

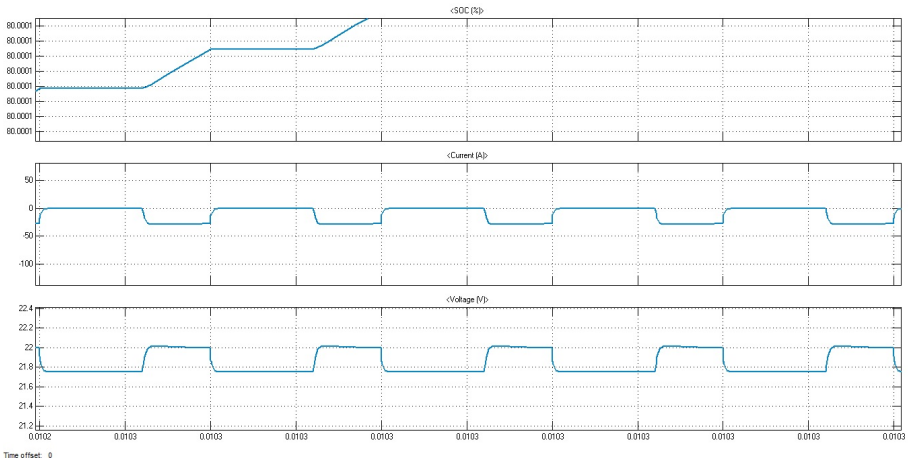

Figure 5.10: Waveform for battery voltage, current and state of charge (SOC) at terminal 2 when duty ratio is changed

Chapter 6

Conclusion and Scope for the Future Work

Chapter 6

Conclusion and Scope for Future work

6.1 Conclusion

In this project the problem for maximizing the power when under varying insolation in series connected PV module has been Studied. Distributed algorithm for differential power processing architecture has been taken under consideration which uses neighbor to neighbor communication to obtain local voltage information is used and perturb and observe algorithm is applied. Simulation has been done to obtain PV module characteristics under varying insolation condition and also open loop Bi-directional buck boost converter is simulated in Simulink to understand the flow of power in both directions.

6.2 Scope for Future work

The PV module is to be implemented on Hardware which should provide the dynamic performance that matches the PV module in outdoor environment. The DPP architecture can be implemented in hardware base with either integrated power stage or discrete power stage and the advantages of both can be observed.

Bibliography

[1] Ren21, Renewables,"Global Status Report, 2011, "(2011): 17-18.

[2] Feldman, David,"Photovoltaic (PV) Pricing Trends: Historical, Recent, and Near-Term Projection,"(2014).

[3] Shenoy, Pradeep S., Katherine A. Kim, and Philip T. Krein,"Comparative Analysis of Differential Power Conversion Architectures and Sontrols for Solar Photovoltaics,"*13th Workshop on Control and Modeling for Power Electronics (COMPEL), IEEE*, 2012.

[4] T. Shimizu, M. Hirakata, T. Kamezawa, and H. Watanabe,"Generation Control Circuit for Photovoltaic Modules,"*IEEE Transactions on Power Electronics*, Vol. 16, (May 2001):293-300.

[5] J. Stauth, M. Seeman, and K. Kesarwani,"A High-Voltage CMOS IC and Embedded System for Distributed Photovoltaic Energy Optimization with Over 99% effective conversion efficiency and insertion loss below 0.1%,"*IEEE International Solid-Stale Circuits Conference*, 2012.

[6] C.Olalla, M. Rodriquez, D. Clement, J. Wang, and D. Maksimovic,"Architecture and Control of PV Modules with Submodule Integrated Converters,"*in Proceedings IEEE Workshop Control, Modeling and Simulation in Power Electronics (COMPEL)*, 2012.

[7] N. Femia, G.Lisi, G.Petrone, G. Spagnuolo, and M. Vitelli,"Distributed Maximum Power Point Tracking of Photovoltaic Arrays: Novel Approach and System Analysis,"*IEEE Transactions on Industrial Electronics*, Vol. 55, No. 7, PP.: 26102621, 2008.

[8] L. Linares, R. Erickson, S. MacAlpine, and M. Brandemuehl,"Improved Energy Capture in Series String Photovoltaics via Smart Distributed Power Electronics,"*in Proceedings of the Applied Power Electronics Conference and Exposition*, (2009): 904910.

[9] R. Pilawa-Podgurski and D. Perreault,"Submodule Integrated Distributed Maximum Power Point Tracking for Solar Photovoltaic Applications,"*IEEE Transactions on Power Electronics*, Vol. 28, No. 6, (2013): 29572967.

[10] Q. Li and P. Wolfs,"A Review of The Single Phase Photovoltaic Module Integrated Converter Topologies with Three Different DC Link Configurations,"*IEEE Transaction on Power Electronics*, Vol. 23, No. 3, pp. 13201333, 2008.

[11] R. Erickson and A. Rogers,"A Micro-Inverter for Building-Integrated Photovoltaics,"*in Proc. of the Applied Power Electronics Conference and Exposition*, pp. 911917, 2009.

[12] A. Trubitsyn, B. Pierquet, A. Hayman, G. Gamache, C. Sullivan, and D. Perreault,"High-Efficiency Inverter for Photovoltaic Applications,"*in Proc. of the Energy Conversion Congress and Exposition*, pp. 28032810, 2010.

[13] H. Field and A. Gabor,"Cell Binning Method Analysis to Minimize Mismatch Losses and Performance Variation in SI-Based Modules,"*in Proc. of the Photovoltaic Specialists Conference*, pp. 418421, 2002.

[14] C. Schaef and J. T. Stauth,"Multilevel Power-Point-Tracking for Variable-Conversion-Ratio Photovoltaic Ladder Converters,"*in Proc. Of the Workshop on Control and Modeling for Power Electronics*, pp. 17, 2013.

[15] I. H. Altas and A.M. Sharaf,"A Photovoltaic Array Simulation Model for Matlab-Simulink GUI Environment,"*IEEE, Clean Electrical Power, International Conference on Clean Electrical Power (ICCEP '07)*, (2007):14-16.

[16] S.Chowdhury, S.P.Chowdhury, G.A.Taylor, and Y.H.Song,"Mathematical Modeling and Performance Evaluation of a Stand-Alone Polycrystalline PV

Plant with MPPT Facility," *IEEE Power and Energy Society General Meeting - Conversion and Delivery of Electrical Energy in the 21st Century*, July 20-24, 2008.

[17] Jee-Hoon Jung, and S. Ahmed,"Model Construction of Single Crystalline Photovoltaic Panels for Real-time Simulation," *IEEE Energy Conversion Congress & Expo*, September 12-16, 2010.

[18] N. Femia , G. Petrone , G. Spagnuolo and M. Vitelli,"A Technique for Improving (P & O) MPPT Performance of Double-Stage Grid-Connected Photovoltaic Systems," *IEEE Transactions in Industrial Electronics*, Vol. 58, No. 11, pp.76 -84 2011.

[19] N. Femia , G. Petrone , G. Spagnuolo and M. Vitelli,"Optimization of Perturb and Observe Maximum Power Point Tracking Method," *IEEE Transactions, Power Electronic*, Vol. 20, No. 4, pp.963 -973 2005.

[20] A. Safari and S. Mekhilef,"Simulation and Hardware Implementation of Incremental Conductance MPPT with Direct Control Method using Cuk Converter," *IEEE Transactions Industrial Electronics*, Vol. 58, No. 4, pp.1154 -1161 2011.

[21] Q. Mei , M. Shan , L. Liuand and J. M. Guerrero,"A Novel Variable Step Size Incremental Resistance MPPT Method for PV Systemsrq ' *IEEE Transactions Industrial Electronics*, Vol. 58, No. 4, pp.2427 -2434 2011.

[22] G.R. Walker, J.K. Xue, and P.C. Sernia,"PV String Permodule Maximum Power Point Enabling Converters," *Proceedings of the Australasian Universities Power Engineering Conference*, 2003. pp. 112117.

[23] S. Singer,"Canonical Approach to Energy Processing Network Synthesis," *IEEE Transactions on Circuits and Systems*, Vol. 33, Aug 1986 pp. 767 774.

[24] H. Xu, X. Wen, E. Qiao, X. Guo, and L. Kong,"High Power Interleaved Boost 131 Converter in Fuel Cell Hybrid Electric Vehicle," *in Proc. IEEE IEMDC*, May 2005, pp. 18141819.

[25] X. Huang, X. Wang, T. Nergaard, J. S. Lai, X. Xu, and L. Zhu,"Parasitic Ringing and Design Issues of Digitally Controlled High Power Interleaved Boost Converters," *IEEE Transactions on Power Electronics*, Vol. 19, No. 5, Sep. 2004, pp.13411352.

[26] Pandiarajan, N., and Ranganath Muthu."Mathematical modeling of photovoltaic module with Simulink." *IEEE Ist International Conference on Electrical energy Systems*, 2011.

[27] Qin, Shibin,et al."A distributed approach to maximum power point tracking for photo voltaic submodule differential power processing." *Power Electronics, IEEE Transactions* , on 30.4 (2015): 2024-2040

[28] Shmilovitz, Doron, and Yoash Levron,"Distributed maximum power point tracking in photovoltaic systemsemerging architectures and control methods," *AUTOMATIKA: asopis za automatiku, mjerenje, elektroniku, raunarstvo i komunikacije 53.2*,(2012): 142-155.

[29] Chao, Kuei-Hsiang, et al."Design and Implementation of a Bidirectional DC-DC Converter for Stand-Alone Photovoltaic Systems." *energy 4* (2013): 8.

[30] Faranda, Roberto, and Sonia Leva."Energy comparison of MPPT techniques for PV Systems." *WSEAS transactions on power systems*,3.6 (2008): 446-455.